Molecular Biology of the Cell
Vol. 10, 2481–2491, August 1999

Distinct Actions and Cooperative Roles of ROCK and mDia in Rho Small G Protein-induced Reorganization of the Actin Cytoskeleton in Madin–Darby Canine Kidney Cells

Katsutoshi Nakano,*† Kenji Takaishi,* Atsuko Kodama,* Akiko Mammoto,* Hitoshi Shiozaki,† Morito Monden,† and Yoshimi Takai*‡

*Department of Molecular Biology and Biochemistry and †Second Department of Surgery, Osaka University Medical School, Suita 565-0871, Japan

Submitted March 10, 1999; Accepted May 17, 1999
Monitoring Editor: Joan Brugge

Rho, a member of the Rho small G protein family, regulates the formation of stress fibers and focal adhesions in various types of cultured cells. We investigated here the actions of ROCK and mDia, both of which have been identified to be putative downstream target molecules of Rho, in Madin–Darby canine kidney cells. The dominant active mutant of RhoA induced the formation of parallel stress fibers and focal adhesions, whereas the dominant active mutant of ROCK induced the formation of stellate stress fibers and focal adhesions, and the dominant active mutant of mDia induced the weak formation of parallel stress fibers without affecting the formation of focal adhesions. In the presence of C3 ADP-ribosyltransferase for Rho, the dominant active mutant of ROCK induced the formation of stellate stress fibers and focal adhesions, whereas the dominant active mutant of mDia induced only the diffuse localization of actin filaments. These results indicate that ROCK and mDia show distinct actions in reorganization of the actin cytoskeleton. The dominant negative mutant of either ROCK or mDia inhibited the formation of stress fibers and focal adhesions, indicating that both ROCK and mDia are necessary for the formation of stress fibers and focal adhesions. Moreover, inactivation and reactivation of both ROCK and mDia were necessary for the 12-*O*-tetradecanoylphorbol-13-acetate–induced disassembly and reassembly, respectively, of stress fibers and focal adhesions. The morphologies of stress fibers and focal adhesions in the cells expressing both the dominant active mutants of ROCK and mDia were not identical to those induced by the dominant active mutant of Rho. These results indicate that at least ROCK and mDia cooperatively act as downstream target molecules of Rho in the Rho-induced reorganization of the actin cytoskeleton.

INTRODUCTION

Rho belongs to the Rho small G protein family and consists of three members RhoA, -B, and -C. Rho regulates the formation of stress fibers and focal adhesions in various types of cultured cells (for review, see Hall, 1994, 1998; Takai *et al.*, 1995). We have been studying the functions of Rho using Madin–Darby canine kidney (MDCK) epithelial cells as a model cell by use of microinjection and stable transfection methods and have shown that Rho regulates not only the formation of stress fibers and focal adhesions but also the localization of the ERM (ezrin, radixin, and moesin) family at the plasma membranes (Kotani *et al.*, 1997; Takaishi *et al.*, 1997). Furthermore, we have shown that activation of Rho is necessary, but not essential, for cadherin-based cell–cell adhesion (Takaishi *et al.*, 1997).

Hepatocyte growth factor/scatter factor is well known to induce scattering of MDCK cells (for review, see Gherardi and Stoker, 1991). We have shown that 12-*O*-tetradecanoylphorbol-13-acetate (TPA), an activator of protein kinase C, also induces scattering of MDCK cells, and that TPA first induces disassembly of stress fibers and focal adhesions, followed by their reassembly in MDCK cells (Takaishi *et al.*, 1995; Imamura *et al.*, 1998). The reassembled stress fibers show radial-like morphology, which is apparently different from the original one. Most reassembled stress fibers run

‡ Corresponding author. E-mail address: ytakai@molbio.med.osaka-u.ac.jp.

Abbreviations used: ERM, ezrin, radixin, and moesin; FH, formin homology; MDCK, Madin–Darby canine kidney; MLC, myosin light chain; TPA, 12-*O*-tetradecanoylphorbol-13-acetate.

radially, whereas most original stress fibers run in parallel. We have shown that inactivation and reactivation of Rho are necessary for the TPA-induced disassembly and reassembly, respectively, of stress fibers and focal adhesions, and that activation of the Rab small G protein family, at least Rab5, is furthermore necessary for their reassembly (Imamura *et al.*, 1998). The Rab family consists of >30 members and regulates intracellular vesicle trafficking (for review, see Simons and Zerial, 1993; Nuoffer and Balch, 1994; Pfeffer, 1994; Novick and Zerial, 1997), and Rab5 regulates early endocytosis (Bucci *et al.*, 1992; Stenmark *et al.*, 1994).

Several putative downstream target molecules of Rho have been identified (for review, see Tapon and Hall, 1997). Among them, ROCK and ROKα, which are mouse and rat counterparts, respectively, regulate the formation of stress fibers and focal adhesions in HeLa cells (Leung *et al.*, 1996, Ishizaki *et al.*, 1997), whereas Rho-kinase, which is a bovine counterpart, regulates the formation of stress fibers and focal adhesions in Swiss 3T3 and MDCK cells (Amano *et al.*, 1997) and phosphorylates and inactivates myosin phosphatase in vitro, thereby regulating myosin light chain (MLC) phosphorylation (Kimura *et al.*, 1996). The ROCK/ROKα/Rho-kinase-induced stress fibers are morphologically different from the Rho-induced ones (Leung *et al.*, 1996; Amano *et al.*, 1997; Ishizaki *et al.*, 1997), suggesting that another downstream target molecule of Rho may be necessary for the entire functions of Rho. The most probable candidate is mDia, because overexpression of full-length mDia induces the formation of actin filaments, which are localized diffusely in COS-7 cells (Watanabe *et al.*, 1997). Moreover, we have isolated mDia from the cytosol fraction of MDCK cells by affinity column chromatography with GST-RhoA with a mutation of amino acid 14 from Gly to Val (V14RhoA) as a ligand (our unpublished results). mDia is a mammalian counterpart of the yeast *Saccharomyces cerevisiae* Bni1p and Bnr1p, which belong to the formin homology (FH) family (for review, see Frazier and Field, 1997). Bni1p is a downstream target molecule of the Rho family members, including Rho1p, Rho3p, Rho4p, and Cdc42p (Kohno *et al.*, 1996; Evangelista *et al.*, 1997; our unpublished results), whereas Bnr1p is a downstream target molecule of Rho4p (Imamura *et al.*, 1997). The FH family proteins are defined by the presence of two FH domains, the proline-rich FH1 domain and the FH2 domain, and have been implicated in cytokinesis and establishment of cell polarity (for review, see Frazier and Field, 1997). Bni1p and Bnr1p directly bind profilin at the FH1 domain, and full-length mDia also binds profilin (Imamura *et al.*, 1997; Watanabe *et al.*, 1997). Profilin is an actin monomer-binding protein and stimulates its polymerization into actin filaments (for review, see Sohn and Goldschmidt-Clermont, 1994).

In this study, we have investigated the roles of ROCK and mDia in the Rho-induced reorganization of the actin cytoskeleton in MDCK cells.

MATERIALS AND METHODS

Materials and Chemicals

MDCK cells were kindly supplied by Dr. W. Birchmeier (Max-Delbruck-Center for Molecular Medicine, Berlin, Germany). TPA was obtained from Sigma Chemical (St. Louis, MO). The cDNAs of mDia and C3, pCAG-*myc*-tagged (pCAG-*myc*) ROCK-Δ1, ROCK-Δ3, and ROCK-KDIA, were provided by Dr. S. Narumiya (Kyoto University Faculty of Medicine, Kyoto, Japan). The cDNA of RhoA was provided by Dr. P. Madaule (Kyoto University Faculty of Medicine). The pEF-BOS expression plasmids were donated from Dr. S. Nagata (Osaka University Medical School, Osaka, Japan). pEF-BOS-*myc*-V14RhoA and pEF-BOS-*myc*-C3 were constructed as described (Komuro *et al.*, 1996). Hybridoma cells expressing the anti-*myc* mouse mAb (9E10) were purchased from American Type Culture Collection (Rockville, MD). The anti-*myc* pAb and the anti-vinculin mouse mAb (V115) were obtained from Medical and Biological Laboratories (Nagoya, Japan) and Sigma, respectively. The anti-E-cadherin rat mAb (ECCD-2) was obtained from Takara Shuzo (Shiga, Japan). The anti-mDia pAb was raised in rabbits by standard procedures using GST-mDia (amino acids 946-1256) as an antigen. The anti-ROCK pAb was obtained from Santa Cruz Biotechnology (Santa Cruz, CA). The anti-ERM family rat mAb was provided by Dr. Sh. Tsukita (Kyoto University Faculty of Medicine). Second antibodies for immunofluorescence microscopy were obtained from Chemicon International (Temecula, CA).

Construction of Expression Plasmids of mDia Mutants

Expression vectors were constructed in pEF-BOS using standard molecular biology methods. Full-length mDia, mDia-ΔC (amino acids 1–571), or mDia-ΔRBDΔC (amino acids 261–571) coding sequence with the *Bgl*II site upstream of the initiation methionine codon and downstream of the termination codon was synthesized by PCR (see Figure 1A). These fragments were digested by *Bgl*II and ligated into the *Bam*HI site of the pEF-BOS-*myc* plasmid. mDia-ΔN (amino acids 524-1256) or mDia-ΔNΔFH1 (amino acids 820-1256) coding sequence with the *Bam*HI site upstream of the initiation methionine codon and downstream of the termination codon was synthesized by PCR (see Figure 1A). These fragments were digested by *Bam*HI and ligated into the *Bam*HI site of the pEF-BOS-*myc* plasmid.

Western Blotting

ROCK and mDia in MDCK cells were detected by Western blotting with the anti-ROCK pAb and the anti-mDia pAb, respectively. Subconfluent monolayers of MDCK cells were lysed in lysis buffer (20 mM Tris-HCl, pH 7.4, containing 150 mM NaCl, 10 mM $MgCl_2$, 1% NP-40, and 100 μM *p*-amidinophenyl methanesulfonyl fluoride). Fifty micrograms of each protein sample from the homogenates were subjected to SDS-PAGE, and the separated proteins were electrophoretically transferred to a nitrocellulose membrane sheet. The sheet was processed to detect ROCK with the anti-ROCK pAb and to detect mDia with the anti-mDia pAb as primary antibodies by using the ECL detection kit (Amersham, Arlington Heights, IL).

Cell Culture, Transfection, and Microinjection

MDCK cells were maintained at 37°C in a humidified atmosphere of 10% CO_2 and 90% air in Dulbecco's modified Eagle's medium containing 10% FCS (Life Technologies, Grand Island, NY), 100 U/ml penicillin, and 100 μg/ml streptomycin. MDCK cells for the microinjection experiments were seeded at a density of 3×10^4 cells per dish onto 35-mm grid dishes. At 24 h after seeding, the expression plasmids were microinjected into the nuclei of the cells at 0.05 mg/ml and then returned to the incubator for 10 h before TPA stimulation or fixation.

Immunofluorescence Microscopy

Cells were fixed in 3.7% paraformaldehyde in PBS for 20 min. The fixed cells were incubated for 10 min with 50 mM ammonium chloride in PBS and permeabilized with PBS containing 0.2% Triton X-100 for 10 min. After the cells were soaked in 10% FCS/PBS for 30

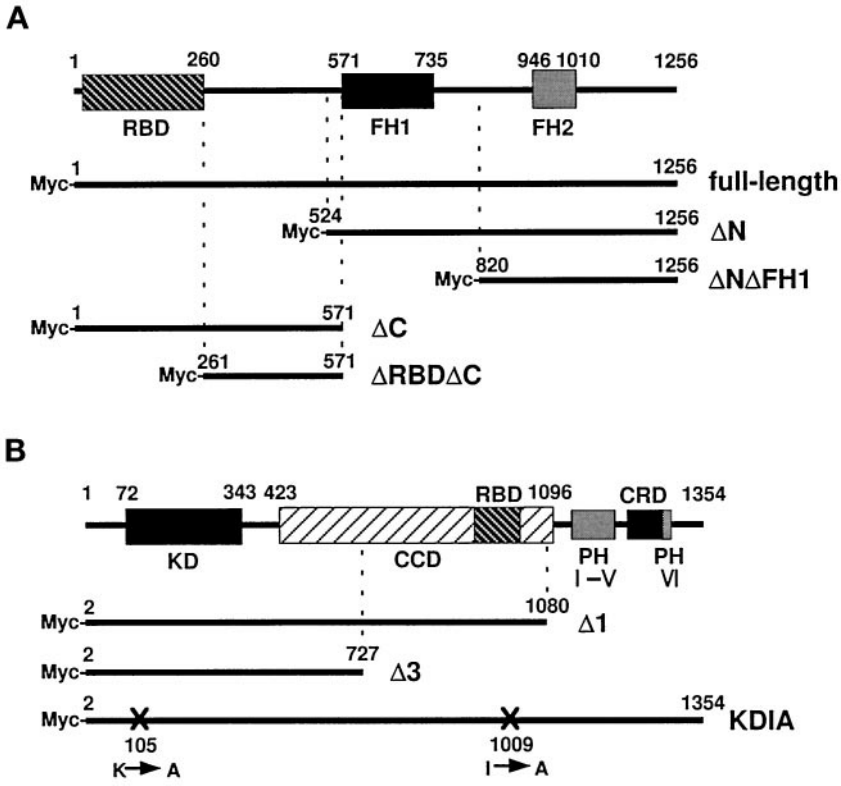

Figure 1. Structures of ROCK, mDia, and their mutants. (A) Structural domains of mDia are schematically illustrated at the top, and full-length and four mutants are represented by the thick lines below. Numbers indicate amino acid residues of the N and C termini of each mutant. RBD, Rho-binding domain; FH1, FH domain 1; FH2, FH domain 2. (B) Structural domains of ROCK are schematically illustrated at the top, and three mutants are represented by the thick lines below. Numbers indicate amino acid residues of the N and C termini of each mutant. KD, kinase domain; CCD, coiled coil–forming amphiphatic α-herical domain; RBD, Rho-binding domain; PH, pleckstrin homology domain; CRD, cysteine-rich zinc-finger domain; X, positions of mutations with amino acid numbers.

min, they were treated with the first antibodies in 10% FCS/PBS for 1 h. The cells were then washed with PBS three times, followed by incubation with the second antibodies in 10% FCS/PBS for 1 h. For the detection of actin filaments, rhodamine-phalloidin was mixed with the second antibody solution. For the double or triple staining, the second antibodies, which did not cross-react with each other, were chosen. After the cells were washed with PBS three times, they were examined using an LSM 410 confocal laser scanning microscope (Carl Zeiss, Oberkochen, Germany).

RESULTS

Construction of Dominant Active and Negative Mutants of mDia and ROCK

We first constructed various expression plasmids encoding full-length or deletion mutants of mDia shown in Figure 1A, all of which had a *myc* tag at the N terminus. mDia-ΔN is expected to act as a dominant active mutant of mDia, whereas mDia-ΔC is expected to act as a dominant negative mutant. The action of mDia-ΔRBDΔC is expected to act as a dominant negative mutant, because we have previously shown that Bni1p interacts with Spa2p at this region, and that this interaction is necessary for the association of Bni1p with the plasma membrane (Fujiwara *et al.*, 1998). mDia-ΔNΔFH1 was constructed to know the function of the FH1 domain.

We used the expression plasmids of ROCK-Δ1, -Δ3, and -KDIA shown in Figure 1B, which were kindly donated by Dr. S. Narumiya. Both ROCK-Δ1 and -Δ3 have been shown to function as dominant active mutants, whereas ROCK-KDIA has been shown to function as a dominant negative mutant (Ishizaki *et al.*, 1997).

Different Morphologies of the Actin Cytoskeleton Induced by Rho, ROCK, and mDia in MDCK Cells

We first examined by Western blotting whether ROCK and mDia are indeed expressed in MDCK cells. In the lysates of MDCK cells, a single band at 160 kDa was detected using the anti-ROCK pAb, and a single band at 170 kDa was detected using the anti-mDia pAb, suggesting the presence of both ROCK and mDia in MDCK cells (our unpublished results).

We then examined the effects of the dominant active mutants of Rho, ROCK, and mDia on the actin cytoskeleton by microinjection of the expression plasmids into the nuclei of MDCK cells. Confocal microscopic analysis at the basal levels showed that wild-type MDCK cells possessed peripheral bundles of actin filaments, which ran at the outer edge of the colonies of the cells, weak actin filaments at the cell–cell adhesion sites, and weak stress fibers as described (Kotani *et al.*, 1997; Imamura *et al.*, 1998) (Figure 2, a and d). Most stress fibers ran in parallel throughout the cells (parallel stress fibers). The staining of vinculin at the basal levels showed the weak dot-like staining, which was localized at the focal adhesions, and the linear staining at the basal edges of the colonies as described (Kotani *et al.*, 1997; Imamura *et al.*, 1998) (Figure 2b). At the junctional levels, the increased localization of actin filaments at the cell–cell adhesion sites was observed in wild-type MDCK cells (Kotani *et al.*, 1997; Imamura *et al.*, 1998) (Figure 2e). The expression of

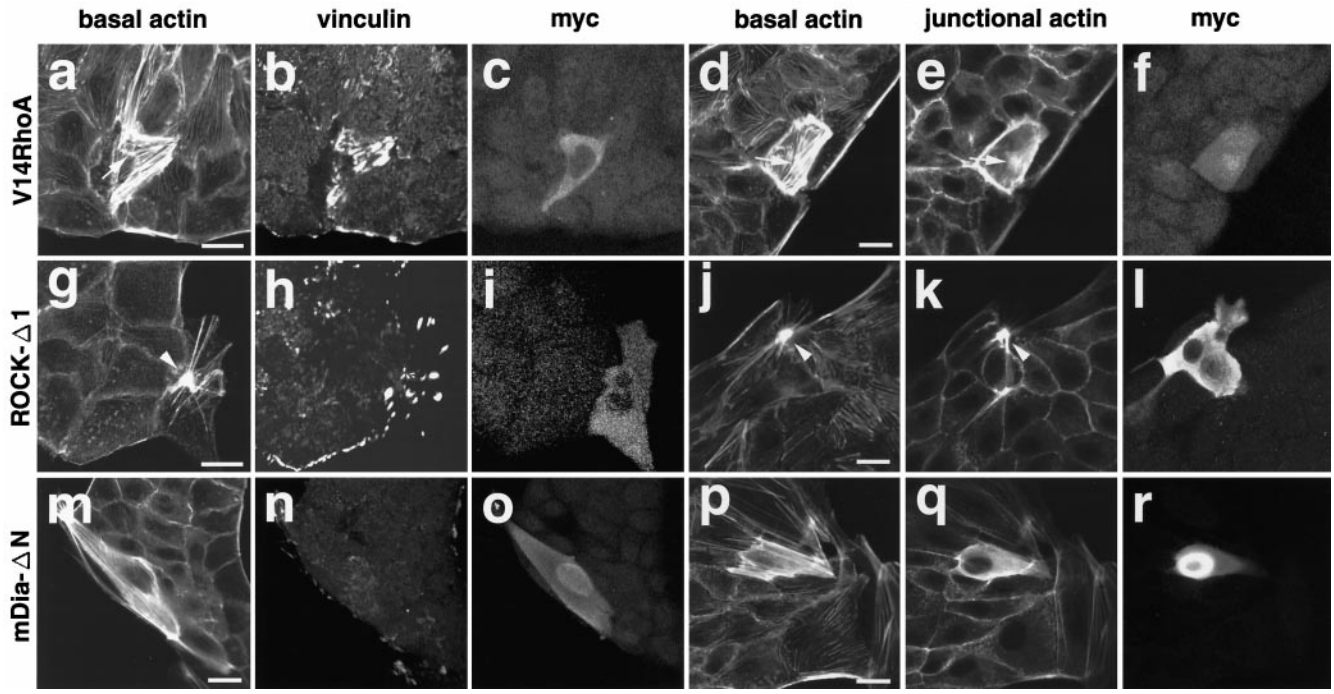

Figure 2. Effect of the dominant active mutant of Rho, ROCK, or mDia on the actin cytoskeleton in MDCK cells. pEF-BOS-*myc*-V14RhoA (a–f), pCAG-*myc*-ROCK-Δ1 (g–l), or pEF-BOS-*myc*-mDia-ΔN (m–r) was microinjected into the nuclei of MDCK cells. At 10 h after the microinjection, the cells were fixed and triple stained with rhodamine-phalloidin (a, g, and m), the anti-vinculin mAb (b, h, and n), and the anti-*myc* pAb (c, i, and o) or double stained with rhodamine-phalloidin (d, e, j, k, p, and q) and the anti-*myc* mAb (f, l, and r). (a–d, g–j, and m–p) Confocal microscopic analysis at the basal levels. (e, f, k, l, q, and r) Confocal microscopic analysis at the junctional levels. The results shown are representative of three independent experiments. Bars, 10 μm. Arrows in a, d, and e indicate the sites where stress fibers coalesced in the V14RhoA-expressing cells. Arrowheads in g, j, and k indicate the sites where stress fibers coalesced in the ROCK-Δ1-expressing cells.

V14RhoA, the dominant active mutant of RhoA, induced the increased formation of stress fibers and the increased staining of vinculin at the focal adhesions (Figure 2, a–f), consistent with our previous results obtained both by microinjection of the guanosine 5′-(3-*O*-thio)-triphosphate-bound form of RhoA into MDCK cells and by stable expression of V14RhoA in MDCK cells (Kotani *et al.*, 1997; Takaishi *et al.*, 1997; Imamura *et al.*, 1998). The V14RhoA-induced stress fibers were relatively thicker than those in wild-type MDCK cells and ran in parallel as those in wild-type MDCK cells, although part of stress fibers coalesced (Figure 2, a and d). The staining of vinculin showed larger dots in the V14RhoA-expressing cells than those in wild-type MDCK cells (Figure 2b). At the junctional levels, the cortical bundles of actin filaments increased in a part of cell–cell adhesion sites (Figure 2e). The increased formation of the cortical bundles was observed in ~40% of the V14RhoA-expressing cells. The staining of actin filaments at the sites, where stress fibers coalesced, was weakly observed at the junctional levels in ~70% of the V14RhoA-expressing cells (Figure 2e).

It has previously been shown that both ROCK-Δ1 and -Δ3, dominant active mutants of ROCK, induce the increased formation of both stress fibers and focal adhesions in HeLa cells, although the ROCK-Δ1- or ROCK-Δ3-induced stress fibers are morphologically different from the V14RhoA-induced ones (Ishizaki *et al.*, 1997). In MDCK cells, overexpression of ROCK-Δ1 also induced the increased formation of both stress fibers and focal adhesions (Figure 2, g–l). The ROCK-Δ1-induced formation of stress fibers was weaker than the V14RhoA-induced one, and the ROCK-Δ1-induced stress fibers were morphologically different from the V14RhoA-induced ones. The ROCK-Δ1-induced stress fibers showed stellate-like morphology (stellate stress fibers) at the basal levels, and the staining of the sites, where stress fibers coalesced, showed dense and large dots at both the basal and junctional levels (Figure 2, g–l). These results are essentially consistent with the previous results obtained in HeLa cells (Ishizaki *et al.*, 1997). The ROCK-Δ1-induced stellate stress fibers coalesced not only at the central region of the cells (Figure 2, g and j) but also at the peripheral region of the cells (our unpublished results). Sometimes, the ROCK-Δ1-induced stellate stress fibers coalesced at the two sites of a single cell (see Figure 3d). The dot-like staining of vinculin at the basal levels increased and became larger (Figure 2h). However, the ROCK-Δ1-induced increased localization of vinculin at the focal adhesions was weaker than the V14RhoA-induced one (Figure 2, b and h). The essentially same results were obtained when ROCK-Δ3 was expressed in MDCK cells (our unpublished results). These results indicate that activation of ROCK induces the increased formation of stress fibers and focal adhesions in MDCK cells, but that the ROCK-induced stress fibers and focal adhesions are morphologically different from the Rho-induced ones.

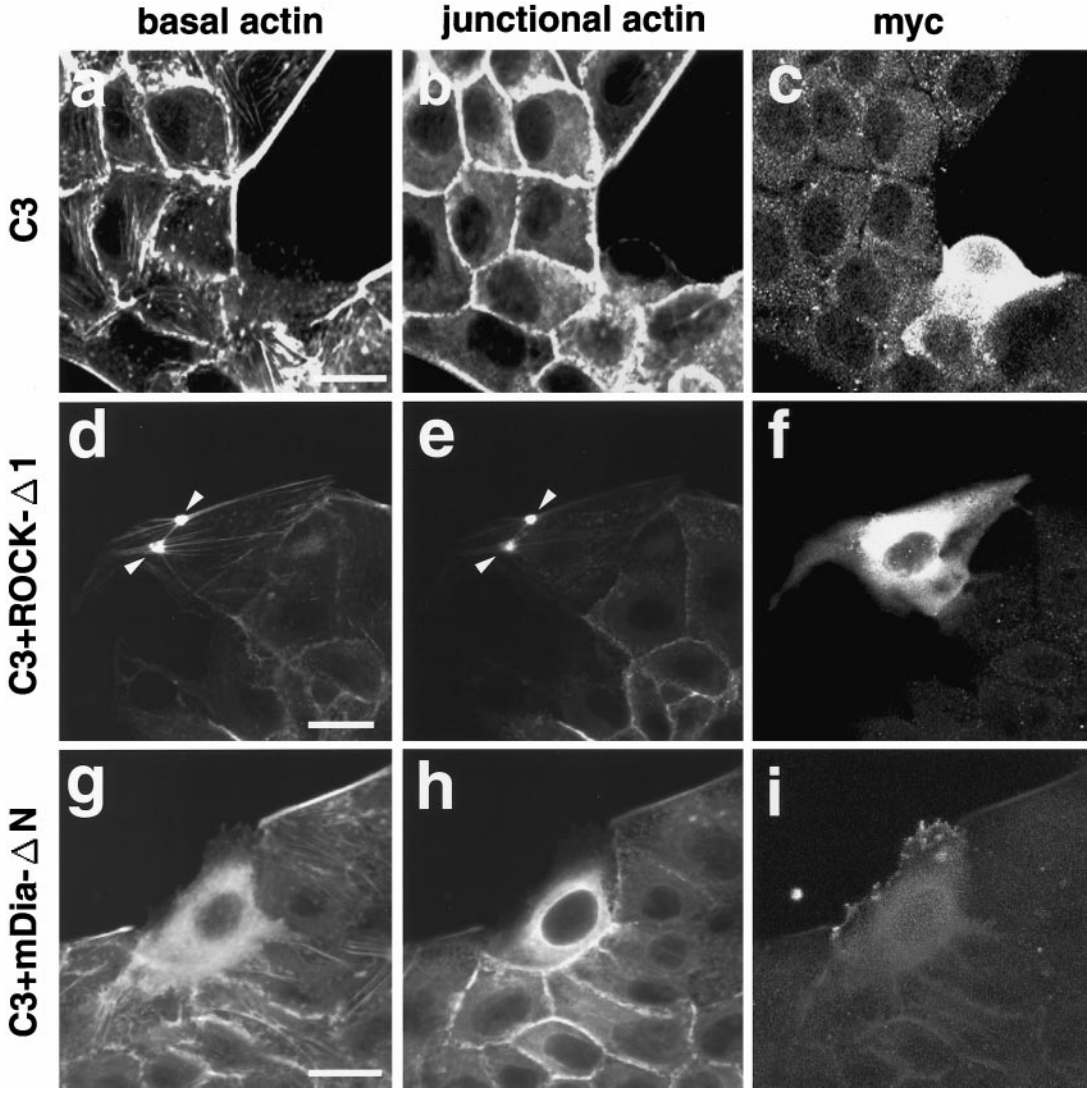

Figure 3. Effect of coexpression of C3 with the dominant active mutant of ROCK or mDia on the actin cytoskeleton in MDCK cells. pEF-BOS-*myc*-C3 (a–c), pEF-BOS-*myc*-C3 plus pCAG-*myc*-ROCK-Δ1 (d–f), and pEF-BOS-*myc*-C3 plus pEF-BOS-*myc*-mDia-ΔN (g–i) were microinjected into the nuclei of MDCK cells. At 10 h after the microinjection, the cells were fixed and double stained with rhodamine-phalloidin (a, b, d, e, g, and h) and the anti-*myc* mAb (c, f, and i). (a, c, d, f, g, and i) Confocal microscopic analysis at the basal levels. (b, e, and h) Confocal microscopic analysis at the junctional levels. The results shown are representative of three independent experiments. Bars, 10 μm. Arrowheads in d and e indicate the sites where stress fibers coalesced in the cells coexpressing C3 and ROCK-Δ1.

It has previously been shown that overexpression of full-length mDia induces the increased formation of actin filaments, which are localized diffusely throughout the cells in COS-7 cells (Watanabe *et al.*, 1997). We first attempted to confirm this result in MDCK cells but did not observe any effect of overexpression of full-length mDia on the actin cytoskeleton in MDCK cells (our unpublished results). However, mDia-ΔN, containing both the FH1 and FH2 domains, induced the weak formation of fine stress fibers, which ran in parallel throughout the cells at the basal levels (Figure 2, m and p). This weak formation of fine stress fibers might be thickening of the preexisting stress fibers. The mDia-ΔN-induced weak stress fibers ran in parallel, but part of the V14RhoA-induced ones coalesced. The number and size of the staining of vinculin at the basal levels did not apparently change in the mDia-ΔN-expressing cells, compared with those in wild-type MDCK cells (Figure 2n). At the junctional levels, the diffuse staining with rhodamine-phalloidin throughout the cells was observed in mDia-ΔN-expressing cells (Figure 2q), and the cortical bundles of actin filaments in a part of cell–cell adhesion sites slightly increased in ~40% of the mDia-ΔN-expressing cells (our unpublished results). *myc*-mDia-ΔN frequently showed the increased staining at the nuclei of the cells, but the physiological significance of this staining is unknown (Figure 2, o and r). These results indicate that the C-terminal region of mDia,

containing both the FH1 and FH2 domains, serves as a dominant active mutant of mDia as expected. It induces the formation of both weak stress fibers, which ran in parallel, and actin filaments, which are localized diffusely throughout the cells, without affecting the formation of focal adhesions. The mDia-induced weak stress fibers and focal adhesions are morphologically different from the Rho- and ROCK-induced ones. We could not apparently observe any effect of mDia-ΔNΔFH1 on the actin cytoskeleton (our unpublished results), indicating that the FH1 domain is essential for these functions of mDia.

Different Morphology of the Actin Cytoskeleton Induced by Coexpression of C3 with ROCK or mDia

The phenotypes of the actin cytoskeleton observed by overexpression of a dominant active mutant of either ROCK or mDia described above were induced under the conditions in which endogenous Rho is likely to function. Therefore, we investigated the effects of ROCK and mDia on the actin cytoskeleton in the presence of C3, which might kill all the functions of endogenous Rho, by comicroinjection of the expression plasmid carrying C3 with those carrying ROCK-Δ1 or mDia-ΔN.

We first examined the effect of C3 alone on the actin cytoskeleton by microinjection of the expression plasmid in MDCK cells. The expression of C3 induced the same effects as obtained by microinjection of C3 (Kotani *et al.*, 1997; Takaishi *et al.*, 1997) that both stress fibers and peripheral bundles disappeared (Figure 3, a–c), that the cell–cell adhesion was disrupted (our unpublished results), and that focal adhesions, the staining of the ERM family at the peripheral bundles, and the staining of vinculin at the basal edges of the colonies disappeared (our unpublished results).

We then examined the effect of coexpression of C3 with ROCK-Δ1 on the actin cytoskeleton. Coexpression of C3 with ROCK-Δ1 induced the formation of stress fibers (Figure 3, d–f) and increased the localization of vinculin at the focal adhesions (our unpublished results), whereas the peripheral bundles disappeared in the cells expressing both C3 and ROCK-Δ1 (our unpublished results). Stress fibers showed stellate-like morphology, and the staining of the sites, where stress fibers coalesced, showed dense and large dots in the cells expressing both C3 and ROCK-Δ1, as observed in the ROCK-Δ1-expressing cells (Figure 3, d–f).

On the other hand, coexpression of C3 with mDia-ΔN induced only the diffuse staining with rhodamine-phalloidin throughout the cells, and the formation of fine stress fibers, which ran in parallel observed in the mDia-ΔN-expressing cells, nearly disappeared by coexpression of C3 (Figure 3, g–i). The formation of the peripheral bundles (Figure 3, g–i) and the staining of vinculin at the focal adhesion (our unpublished results) also disappeared in the cells expressing both C3 and mDia-ΔN.

These results indicate that activation of ROCK alone induces the formation of stellate stress fibers and focal adhesions, whereas activation of mDia alone induces only the formation of actin filaments, which are localized diffusely throughout the cells.

Involvement of Both ROCK and mDia in the Formation of Stress Fibers and Focal Adhesions

We examined by use of dominant negative mutants of ROCK and mDia whether both the downstream target molecules of Rho are involved in the formation of stress fibers and focal adhesions in MDCK cells. ROCK-KDIA, containing double mutations at both the kinase domain and the Rho-binding domain, has been shown to act as a dominant negative mutant of ROCK and to inhibit the formation of stress fibers and focal adhesions in HeLa cells (Ishizaki *et al.*, 1997). Overexpression of ROCK-KDIA in MDCK cells diminished both stress fibers (Figure 4A, a–c) and the staining of vinculin at focal adhesions (our unpublished results) at the basal levels. Moreover, the cell–cell adhesion was partially disrupted (Figure 4A, b), and a part of the localization of E-cadherin at the cell–cell adhesion sites disappeared in the ROCK-KDIA-expressing cells (Figure 4B, a and b). The expression of ROCK-KDIA also diminished the peripheral bundles (our unpublished results) and inhibited the localization of the ERM family at the peripheral bundles (Figure 4B, c and d) and vinculin at the basal edges of the colonies (our unpublished results). These changes in the actin cytoskeleton induced by ROCK-KDIA were similar to those induced by C3 (Kotani *et al.*, 1997; Takaishi *et al.*, 1997).

Overexpression of mDia-ΔC in MDCK cells induced the same changes in the actin cytoskeleton as those observed in the C3- or ROCK-KDIA-expressing cells (our unpublished results). Because mDia-ΔC contains the Rho-binding domain, the effect of mDia-ΔC on the actin cytoskeleton may be simply due to the competitive inhibition of binding of endogenous mDia to Rho. However, we found that overexpression of mDia-ΔRBDΔC in MDCK cells also inhibited the formation of stress fibers (Figure 4A, d–f) and focal adhesions (our unpublished results), indicating that mDia-ΔRBDΔC acts as a dominant negative mutant. mDia-ΔRBDΔC did not induce the disruption of cell–cell adhesion (Figure 4A, e) or loss of the staining of E-cadherin at the cell–cell adhesion sites (Figure 4B, e and f). mDia-ΔRBDΔC also did not induce the disappearance of the peripheral bundles (our unpublished results) or loss of the staining of the ERM family at the peripheral bundles (Figure 4B, g and h) and vinculin at the basal edge of the colonies (our unpublished results).

These results indicate that activation of both ROCK and mDia is necessary for the formation of stress fibers and focal adhesions and that activation of ROCK, but not mDia, is necessary for the formation of cell–cell adhesion and the peripheral bundles and the localization of the ERM family and vinculin at the peripheral bundles and the basal edge of the colonies, respectively.

Cooperative Roles of ROCK and mDia in the Rho-induced Reorganization of the Actin Cytoskeleton

The ROCK- or mDia-induced stress fibers and focal adhesions are morphologically different from the Rho-induced ones, although activation of both ROCK and mDia is necessary for the formation of these structures as described above. We examined the effect of coexpression of ROCK-Δ1 and mDia-ΔN on the morphologies of stress fibers and focal adhesions, on the assumption that, if the Rho-induced formation of stress fibers and focal adhesions is simply medi-

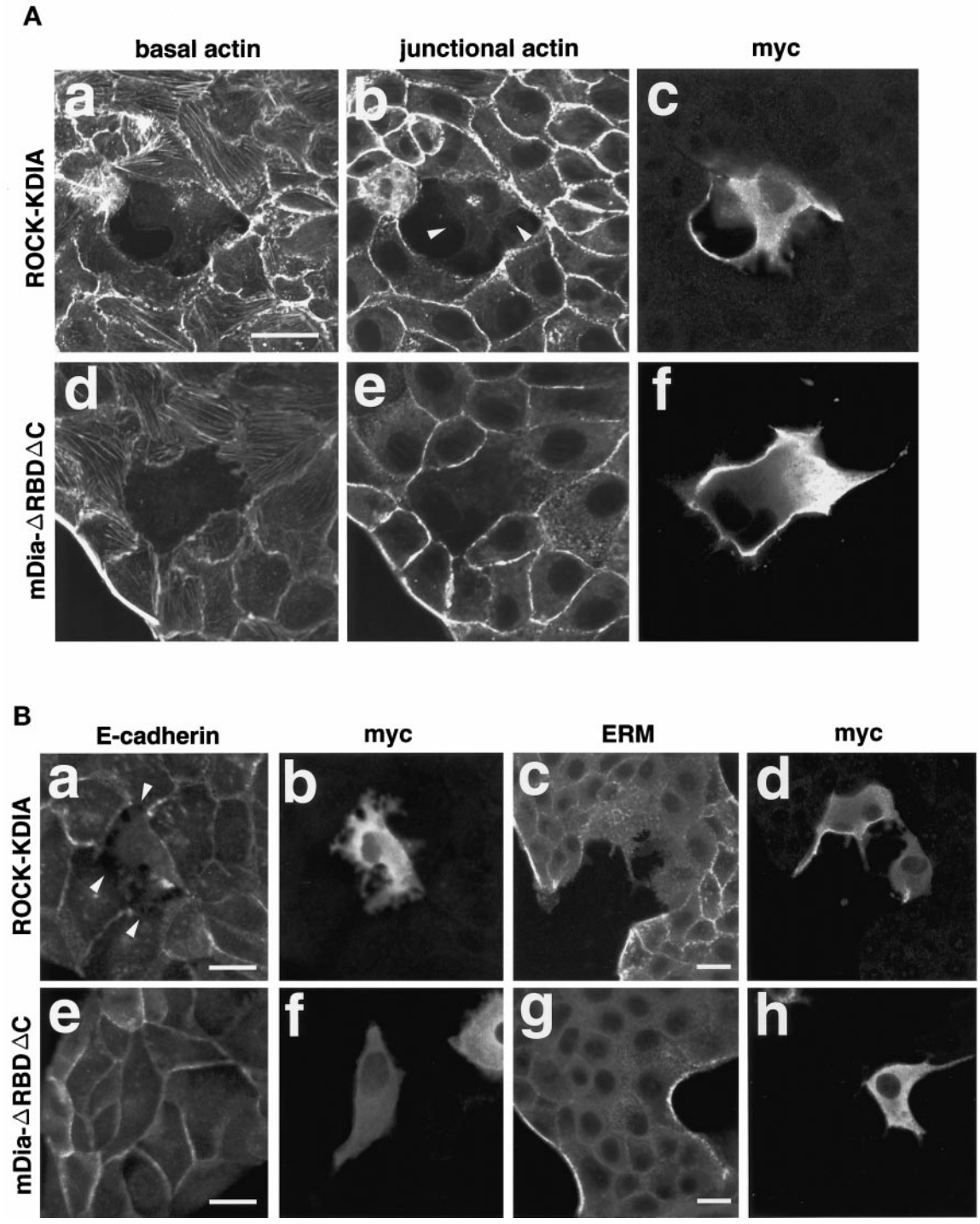

Figure 4. Effect of the dominant negative mutant of ROCK or mDia on the actin cytoskeleton, E-cadherin, and the ERM family in MDCK cells. (A) pCAG-*myc*-ROCK-KDIA (a–c) and pEF-BOS-*myc*-mDia-ΔRBDΔC (d–f) were microinjected into the nuclei of MDCK cells. At 10 h after the microinjection, the cells were fixed and double stained with rhodamine-phalloidin (a, b, d, and e) and the anti-*myc* mAb (c and f). (a and d) Confocal microscopic analysis at the basal levels. (b, c, e, and f) Confocal microscopic analysis at the junctional levels. (B) pCAG-*myc*-ROCK-KDIA (a–d) and pEF-BOS-*myc*-mDia-ΔRBDΔC (e–h) were microinjected into the nuclei of MDCK cells. At 10 h after the microinjection, the cells were fixed and double stained with the ECCD-2 anti-E-cadherin mAb (a and e) and the anti-*myc* mAb (b and f) or with the anti-ERM family mAb (c and g) and the anti-*myc* mAb (d and h) and analyzed at the junctional levels using confocal microscopy. The results shown are representative of three independent experiments. Bars, 10 μm. Arrowheads in A, b, indicate the sites where cell–cell adhesion is disrupted. Arrowheads in B, a, indicate the sites where the staining of E-cadherin at the cell–cell adhesion sites disappeared.

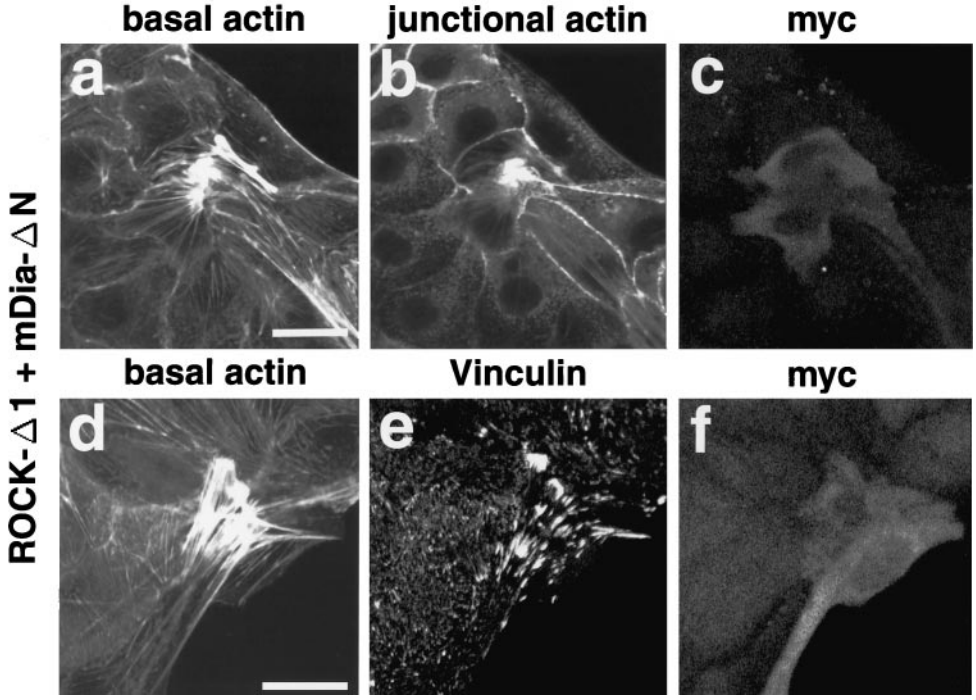

Figure 5. Effect of coexpression of ROCK and mDia on the actin cytoskeleton in MDCK cells. pCAG-*myc*-ROCK-Δ1 plus pEF-BOS-*myc*-mDia-ΔN were microinjected into the nuclei of MDCK cells. At 10 h after the microinjection, the cells were fixed and double stained with rhodamine-phalloidin (a and b) and the anti-*myc* mAb (c) or triple stained with rhodamine-phalloidin (d), the anti-vinculin mAb (e), and the anti-*myc* pAb (f). (a, d, e, and f) Confocal microscopic analysis at the basal levels. (b and c) Confocal microscopic analysis at the junctional levels. The results shown are representative of three independent experiments. Bars, 10 μm.

ated by the activation of both ROCK and mDia, their morphologies in the cells coexpressing ROCK-Δ1 and mDia-ΔN may resemble the V14RhoA-induced ones. Coexpression of both the proteins induced the formation of stress fibers that were stronger than those in the cells expressing either ROCK-Δ1 or mDia-ΔN alone (Figure 5, a, c, d, and f). The stress fibers morphologically resembled the stellate type rather than the parallel type, and the sites, where stress fibers coalesced, were densely stained (Figure 5, a and d). The staining of the sites, where stress fibers coalesced, was also observed at the junctional levels, and the staining of the sites, where stress fibers coalesced, showed apparently larger dots than that in the ROCK-Δ1-expressing cells (Figure 5b). The staining of vinculin at the focal adhesion increased, compared with that in the ROCK-Δ1-expressing cells (Figure 5e). These results indicate that the morphologies of stress fibers and focal adhesions induced by coexpression of ROCK and mDia are not identical to the Rho-induced ones.

Involvement of Both ROCK and mDia in the TPA-induced Reorganization of the Actin Cytoskeleton

We have previously shown that TPA induces disassembly of stress fibers and focal adhesions at 15 min, followed by their reassembly at 2 h in MDCK cells (Takaishi *et al.*, 1995; Imamura *et al.*, 1998), and that inactivation and activation of Rho are necessary for the TPA-induced disassembly and reassembly, respectively, of stress fibers and focal adhesions (Imamura *et al.*, 1998). The reassembled stress fibers are morphologically different from the original ones (Takaishi *et al.*, 1995; Imamura *et al.*, 1998). Most reassembled stress fibers run radially, whereas most original stress fibers run in parallel. We investigated the effect of the expression plasmid carrying V14RhoA or C3 on the TPA-induced reorganization of the actin cytoskeleton by microinjection of the expression plasmids into the nuclei of MDCK cells. The TPA-induced disassembly of stress fibers (Figure 6, a and b) and focal adhesions (our unpublished results) was not induced in the V14RhoA-expressing cells at 15 min after TPA stimulation. The stress fibers in the V14RhoA-expressing cells at 15 min after TPA stimulation morphologically resembled those in the V14RhoA-expressing cells without TPA stimulation. The stress fibers in the V14RhoA-expressing cells at 2 h after TPA stimulation also morphologically resembled those in the V14RhoA-expressing cells without TPA stimulation and were apparently different from the TPA-induced ones (Figure 6, c and d). These results are consistent with our previous results obtained using the MDCK cell lines stably expressing V14RhoA (Imamura *et al.*, 1998). Overexpression of C3 inhibited the TPA-induced reassembly of stress fibers (Figure 6, e and f) and focal adhesions (our unpublished results) at 2 h after TPA stimulation, and this result is consistent with our previous result obtained by microinjection of C3 (Imamura *et al.*, 1998). These results indicate that inactivation and reactivation of Rho are necessary for the TPA-induced disassembly and reassembly, respectively, of stress fibers and focal adhesions in MDCK cells.

We next examined the effects of the ROCK and mDia mutants on the TPA-induced reorganization of the actin cytoskeleton. Overexpression of ROCK-Δ1 inhibited the TPA-induced disassembly of stress fibers (Figure 6, g and h) and focal adhesions (our unpublished results). The stellate stress fibers were observed in the ROCK-Δ1-expressing cells at 15 min after TPA stimulation and morphologically resembled those in the ROCK-Δ1-expressing cells without TPA stimulation. At 2 h after TPA stimulation, the formation of

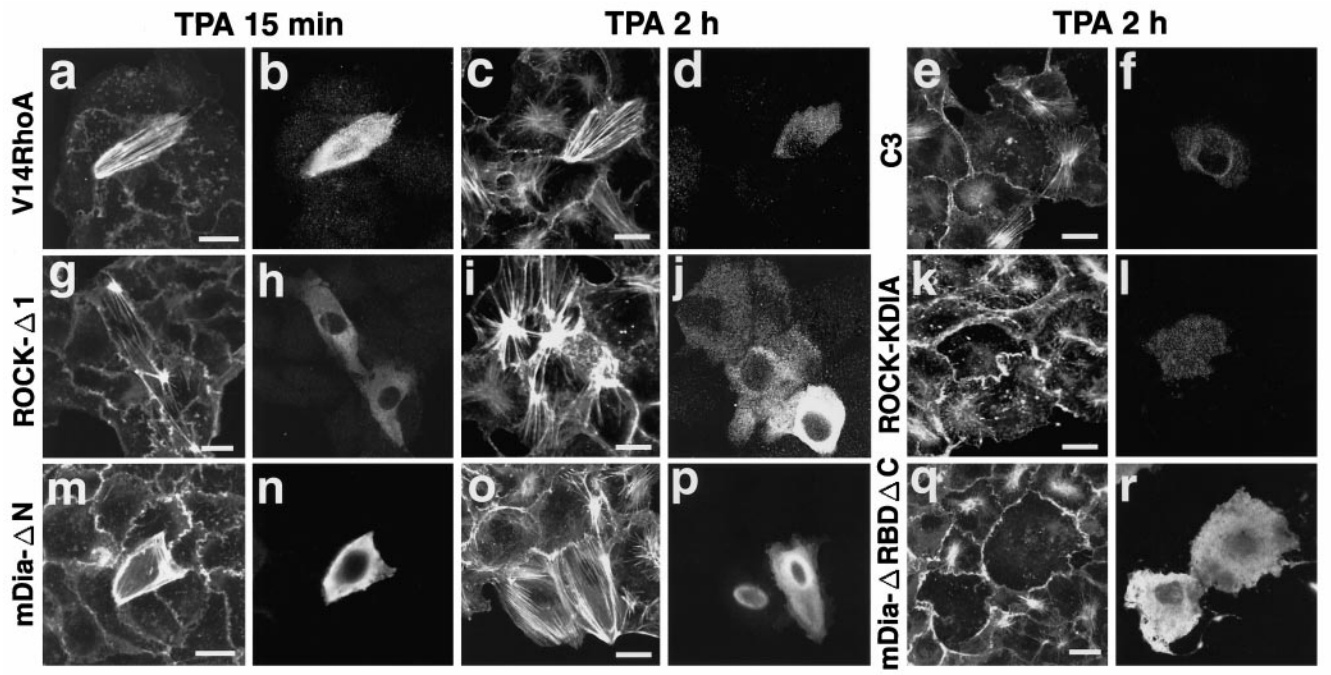

Figure 6. Effect of ROCK and mDia mutants on the TPA-induced reorganization of the actin cytoskeleton in MDCK cells. pEF-BOS-*myc*-V14RhoA (a–d), pEF-BOS-*myc*-C3 (e and f), pCAG-*myc*-ROCK-Δ1 (g–j), pCAG-*myc*-ROCK-KDIA (k and l), pEF-BOS-*myc*-mDia-ΔN (m–p), or pEF-BOS-*myc*-mDia-ΔRBDΔC (q and r) were microinjected into the nuclei of MDCK cells. At 10 h after the microinjection, the cells were stimulated with 100 nM TPA for 15 min (a, b, g, h, m, and n) or 2 h (c–f, i–l, and o–r) and fixed. The cells were double stained with rhodamine-phalloidin (a, c, e, g, i, k, m, o, and q) and the anti-*myc* mAb (b, d, f, h, j, l, n, p, and r) and analyzed at the basal levels using confocal microscopy. The results shown are representative of three independent experiments. Bars, 10 μm.

stellate stress fibers increased in the ROCK-Δ1-expressing cells, but the stress fibers in the ROCK-Δ1-expressing cells were not morphologically identical to those in wild-type MDCK cells (Figure 6, i and j). The staining of the sites, where stellate stress fibers coalesced in the ROCK-Δ1-expressing cells, showed slightly smaller and denser dots than that in wild-type cells. Overexpression of ROCK-KDIA inhibited the TPA-induced reassembly of stress fibers (Figure 6, k and l) and focal adhesions (our unpublished results) at 2 h after TPA stimulation. These results indicate that inactivation and reactivation of ROCK are necessary for the TPA-induced disassembly and reassembly, respectively, of stress fibers and focal adhesions.

Overexpression of mDia-ΔN induced the formation of fine stress fibers, which ran in parallel, and actin filaments, which were localized diffusely throughout the cells, but did not affect the formation of focal adhesions as described above. The formation of parallel stress fibers in the mDia-ΔN-expressing cells at 15 min after TPA stimulation became slightly weaker than that without stimulation but was still observed (Figure 6, m and n). The formation of focal adhesions in the mDia-ΔN-expressing cells at 15 min after TPA stimulation also became slightly weaker than that without stimulation but was still observed (our unpublished results). The formation of parallel stress fibers in the mDia-ΔN-expressing cells at 2 h after TPA stimulation became stronger again (Figure 6, o and p). The formation of parallel stress fibers in the mDia-ΔN-expressing cells at 2 h after TPA stimulation was stronger than that without TPA stimulation, and stress fibers in the mDia-ΔN-expressing cells at 2 h after TPA stimulation were slightly thicker than those without stimulation (Figure 6, o and p). The formation of focal adhesions in the mDia-ΔN-expressing cells at 2 h after TPA stimulation was also stronger than that without TPA stimulation (our unpublished results). Overexpression of mDia-ΔRBDΔC inhibited the TPA-induced reassembly of stress fibers (Figure 6, q and r) and focal adhesions (our unpublished results) at 2 h after TPA stimulation. These results indicate that inactivation and reactivation of mDia are necessary for the TPA-induced disassembly and reassembly, respectively, of stress fibers and focal adhesions.

DISCUSSION

We have shown here by use of dominant active and negative mutants of ROCK and mDia, downstream target molecules of Rho, that they have distinct but cooperative roles in the Rho-induced reorganization of the actin cytoskeleton in MDCK cells. The morphologies of stress fibers and focal adhesions induced by either ROCK-Δ1 or mDia-ΔN are different from the V14RhoA-induced ones, and those induced by coexpression of ROCK-Δ1 and mDia-ΔN are not identical to the V14RhoA-induced ones, either, but more similar to the ROCK-Δ1-induced ones. These results indicate that another downstream target molecule of Rho may also be necessary for the Rho-induced reorganization of the actin cytoskeleton. It is also possible that the different morphologies

of stress fibers between the cells coexpressing ROCK-Δ1 and mDia-ΔN and the V14RhoA-expressing cells may be due to the different activities of ROCK and mDia. If the expression level of ROCK-Δ1 is higher than that of mDia in the cells expressing both ROCK-Δ1 and mDia-ΔN, the stress fibers may morphologically resemble the ROCK-Δ1-induced ones.

We have shown here that the morphology of ROCK-induced stellate stress fibers is different from that of the TPA-induced radial stress fibers in wild-type MDCK cells, but the stress fibers in the ROCK-Δ1-expressing cells stimulated by TPA are morphologically similar, but not identical, to the radial stress fibers in wild-type MDCK cells stimulated by TPA. The precise mechanisms of the TPA-induced reassembly of stress fibers and focal adhesions are not known, but these results suggest that ROCK may be involved in the TPA-induced reassembly of stress fibers and focal adhesions as a main downstream target molecule of Rho. We have previously found that activation of not only Rho but also some Rab family members, at least Rab5, is necessary for the TPA-induced reassembly of stress fibers and focal adhesions (Imamura *et al.*, 1998). ROCK may cooperate with some Rab family members, at least Rab5, in the formation of radial stress fibers and focal adhesions. It may be noted that the morphologies of stress fibers in wild-type cells without TPA stimulation and the V14RhoA-expressing cells show parallel type, whereas those in wild-type cells at 2 h after TPA stimulation show radial type. mDia may mainly function in wild-type cells without TPA stimulation and the V14RhoA-expressing cells, whereas ROCK may mainly function in wild-type cells at 2 h after TPA stimulation.

We have shown here that all the changes in the actin cytoskeleton induced by ROCK-KDIA are similar to those induced by C3 (Kotani *et al.*, 1997; Takaishi *et al.*, 1997), suggesting that activation of ROCK alone is necessary, but not sufficient, for all the actions of Rho in MDCK cells. In the case of mDia-ΔRBDΔC, it does not induce the disruption of the E-cadherin-based cell–cell adhesion or inhibit the formation of the peripheral bundles and the localization of the ERM family and vinculin at the peripheral bundles and the basal edges of the colonies, respectively, suggesting that activation of mDia is not necessary for these functions of Rho, in contrast to the actions of C3 and ROCK-KDIA. We have previously shown that C3 induces the disappearance of stress fibers and focal adhesions, followed by the disruption of cell–cell adhesion and cell rounding, suggesting that the C3-induced loss of stress fibers, focal adhesions, and normal cell shape secondarily disrupts the cell–cell adhesion (Takaishi *et al.*, 1997). The ROCK-KDIA-induced disruption of cell–cell adhesion is likely due to the same mechanism as that of C3. The inability of mDia-ΔRBDΔC to affect the cell–cell adhesion may be due to its inability to affect the formation of focal adhesions.

The mode of action of ROCK in the Rho-induced reorganization of the actin cytoskeleton has not fully been understood, but Rho kinase has been shown to phosphorylate and inactivate myosin phosphatase in vitro, thereby regulating MLC phosphorylation (Kimura *et al.*, 1996). The ROCK-induced stellate stress fibers, which coalesce densely, may result from contraction of the actomyosin system through elevated MLC phosphorylation, whereas the ROCK-induced formation of focal adhesions may be mediated through another mechanism.

The mode of action of mDia in the Rho-induced reorganization of the actin cytoskeleton has not fully been understood, either, but mDia contains many functional domains, including the FH1 and FH2 domains. It has previously been shown that full-length mDia induces diffuse localization of actin filaments in COS-7 cells (Watanabe *et al.*, 1997). However, we have not apparently observed any effect of full-length mDia on the actin cytoskeleton in MDCK cells. This result is inconsistent with the previous result, but this discrepancy may be due to the difference in the expression levels of mDia in our and their systems. Our results that mDia-ΔN lacking the Rho-binding domain, but not full-length mDia, affects the actin cytoskeleton suggest that the Rho-binding domain shows an inhibitory effect on the function of mDia. We have found that mDia-ΔNΔFH1 does not apparently show any effect on the actin cytoskeleton, suggesting that the FH1 domain is essential for the function of mDia. It has been shown that full-length mDia binds profilin, which is involved in actin polymerization (Watanabe *et al.*, 1997), but the profilin-binding region of mDia has not been studied. Because we have shown that yeast Bni1p and Bnr1p bind profilin at the proline-rich FH1 domain (Imamura *et al.*, 1997), mDia is likely to bind profilin also at this FH1 domain. Moreover, the association of profilin with proline-rich domain of neural Wiscott–Aldrich syndrome protein, a downstream target molecule of Cdc42, is essential for actin polymerization in microspike formation (Suetsugu *et al.*, 1998). Taken together, mDia is most likely to induce the formation of actin filaments at least through profilin. The mechanism that mDia-ΔRBDΔC acts as a dominant negative mutant is not known, but because Bni1p, a yeast counterpart of mDia, interacts with Spa2p at this region, and this interaction is essential for the association of Bni1p with the plasma membrane (Fujiwara *et al.*, 1998), mDia may also be associated with the plasma membrane through a Spa2-like protein, and mDia-ΔRBDΔC may compete with endogenous mDia for the binding of this protein to the plasma membrane. It is also possible that mDia-ΔRBDΔC binds the Rho-binding domain of mDia and abolishes the function of endogenous mDia, because this region of Bni1p intramoleculary or intermoleculary binds the Rho-binding domain of Bni1p (our unpublished results).

We have shown here that mDia-ΔN induces the formation of parallel stress fibers in the cells without stimulation or with TPA stimulation for 2 h. If mDia regulates simply the formation of actin filaments, another structure of actin filaments such as membrane ruffles may be formed in the mDia-ΔN-expressing cells without TPA stimulation, and radial stress fibers may be formed in the mDia-ΔN-expressing cells at 2 h after TPA stimulation. However, mDia-ΔN does not form these structures. Therefore, it is likely that mDia has another function to first recruit the newly formed actin filaments to stress fibers, but not membrane ruffles, and then induce the morphology of stress fibers in parallel. Furthermore, the FH2 domain, of which function is not known, or another region of mDia-ΔN may be important for the entire functions of mDia.

ACKNOWLEDGMENTS

We thank Dr. W. Birchmeier for providing MDCK cells, Dr. P. Madaule for the cDNA of RhoA, Dr. S. Nagata for the pEF-BOS expression plasmid, Dr. S. Narumiya for the cDNAs of mDia and C3 and the expression plasmids of pCAG-*myc*-ROCK-Δ1, ROCK-Δ3, and ROCK-KDIA, and Dr. Sh. Tsukita for the anti-ERM family rat mAb. This investigation was supported by grants-in-aid for scientific research and for cancer research from the Ministry of Education, Science, Sports, and Culture, Japan (1998) and by grants from the Human Frontier Science Program (1998).

REFERENCES

Amano, M., Chihara, K., Kimura, K., Fukata, Y., Nakamura, N., Matsuura, Y., and Kaibuchi, K. (1997). Formation of actin stress fibers and focal adhesions enhanced by Rho-kinase. Science *275*, 1308–1311.

Bucci, C., Parton, R.G., Mather, I.H., Stunnenberg, H., Simons, K., Hoflack, B., and Zerial, M. (1992). The small GTPase rab5 functions as a regulatory factor in the early endocytic pathway. Cell *70*, 715–728.

Evangelista, M., Blundell, K., Longtine, M.S., Chow, C.J., Adames, N., Pringle, J.R., Peter, M., and Boone, C. (1997). Bni1p, a yeast formin linking Cdc42p and the actin cytoskeleton during polarized morphogenesis. Science *276*, 118–122.

Frazier, J.A., and Field, C.M. (1997). Actin cytoskeleton: are FH proteins local organizers? Curr. Biol. *7*, R414–R417.

Fujiwara, T., Tanaka, K., Mino, A., Kikyo, M., Takahashi, K., Shimizu, K., and Takai, Y. (1998). Rho1p-Bni1p-Spa2p interactions: implication in localization of Bni1p at the bud site and regulation of the actin cytoskeleton in *Saccharomyces cerevisiae*. Mol. Biol. Cell *9*, 1221–1233.

Gherardi, E., and Stoker, M. (1991). Hepatocyte growth factor-scatter factor: mitogen, motogen, and Met. Cancer Cells *3*, 227–232.

Hall, A. (1994). Small GTP-binding proteins and the regulation of the actin cytoskeleton. Annu. Rev. Cell Biol. *10*, 31–54.

Hall, A. (1998). Rho GTPases and the actin cytoskeleton. Science *279*, 509–514.

Imamura, H., Takaishi, K., Nakano, K., Kodama, A., Oishi, H., Shiozaki, H., Monden, M., Sasaki, T., and Takai, Y. (1998). Rho and Rab small G proteins coordinately reorganize stress fibers and focal adhesions in MDCK cells. Mol. Biol. Cell *9*, 2561–2575.

Imamura, H., Tanaka, K., Hihara, T., Umikawa, M., Kamei, T., Takahashi, K., Sasaki, T., and Takai, Y. (1997). Bni1p and Bnr1p: downstream targets of the Rho family small G-proteins which interact with profilin and regulate actin cytoskeleton in *Saccharomyces cerevisiae*. EMBO J. *16*, 2745–2755.

Ishizaki, T., Naito, M., Fujisawa, K., Maekawa, M., Watanabe, N., Saito, Y., and Narumiya, S. (1997). $p160^{ROCK}$, a Rho-associated coiled-coil forming protein kinase, works downstream of Rho and induces focal adhesions. FEBS Lett. *404*, 118–124.

Kimura, K., *et al*. (1996). Regulation of myosin phosphatase by Rho and Rho-associated kinase (Rho-kinase). Science *273*, 245–248.

Kohno, H., *et al*. (1996). Bni1p implicated in cytoskeletal control is a putative target of Rho1p small GTP binding protein in *Saccharomyces cerevisiae*. EMBO J. *15*, 6060–6068.

Komuro, R., Sasaki, T., Takaishi, K., Orita, S., and Takai, Y. (1996). Involvement of Rho and Rac Small G proteins and Rho GDI in Ca^{2+}-dependent exocytosis from PC12 cells. Genes Cells *1*, 943–951.

Kotani, H., Takaishi, K., Sasaki, T., and Takai, Y. (1997). Rho regulates association of both the ERM family and vinculin with the plasma membrane in MDCK cells. Oncogene *14*, 1705–1713.

Leung, T., Chen, X.Q., Manser, E., and Lim, L. (1996). The p160 RhoA-binding kinase ROKα is a member of a kinase family and is involved in the reorganization of the cytoskeleton. Mol. Cell. Biol. *16*, 5313–5327.

Novick, P., and Zerial, M. (1997). The diversity of Rab proteins in vesicle transport. Curr. Opin. Cell Biol. *9*, 496–504.

Nuoffer, C., and Balch, W.E. (1994). GTPases: multifunctional molecular switches regulating vesicular traffic. Annu. Rev. Biochem. *63*, 949–990.

Pfeffer, S.R. (1994). Rab GTPases: master regulators of membrane trafficking. Curr. Opin. Cell Biol. *6*, 522–526.

Simons, K., and Zerial, M. (1993). Rab proteins and the road maps for intracellular transport. Neuron *11*, 789–799.

Sohn, R.H., and Goldschmidt-Clermont, P.J. (1994). Profilin: at the cross-roads of signal transduction and the actin cytoskeleton. Bioessays *16*, 465–472.

Stenmark, H., Parton, R.G., Steele-Mortimer, O., Lutcke, A., Gruenberg, J., and Zerial, M. (1994). Inhibition of rab5 GTPase activity stimulates membrane fusion in endocytosis. EMBO J. *13*, 1287–1296.

Suetsugu, S., Miki, H., and Takenawa, T. (1998). The essential role of profilin in the assembly of actin for microspike formation. EMBO J. *17*, 6516–6526.

Takai, Y., Sasaki, T., Tanaka, K., and Nakanishi, H. (1995). Rho as a regulator of the cytoskeleton. Trends Biochem. Sci. *20*, 227–231.

Takaishi, K., Sasaki, T., Kameyama, T., Tsukita, Sa., Tsukita, Sh., and Takai, Y. (1995). Translocation of activated *Rho* from the cytoplasm to membrane ruffling area, cell-cell adhesion sites and cleavage furrows. Oncogene *11*, 39–48.

Takaishi, K., Sasaki, T., Kotani, H., Nishioka, H., and Takai, Y. (1997). Regulation of cell-cell adhesion by Rac and Rho small G proteins in MDCK cells. J. Cell Biol. *139*, 1047–1059.

Tapon, N., and Hall, A. (1997). Rho, Rac and Cdc42 GTPases regulate the organization of the actin cytoskeleton. Curr. Opin. Cell Biol. *9*, 86–92.

Watanabe, N., Madaule, P., Reid, T., Ishizaki, T., Watanabe, G., Kakizuka, A., Saito, Y., Nakao, K., Jockusch, B.M., and Narumiya, S. (1997). p140mDia, a mammalian homolog of *Drosophila* diaphanous, is a target protein for Rho small GTPase and is a ligand for profilin. EMBO J. *16*, 3044–3056.